Strain Effects on Electronic Bandstructures in Nanoscaled Silicon: From Bulk to Nanowire

Maegawa, Tadashi
Yamauchi, Tsuneki
Hara, Takeshi
Tsuchiya, Hideaki
Ogawa, Matsuto

(Citation)
IEEE Transactions on Electron Devices,56(4):553-559

(Issue Date)
2009-04

(Resource Type)
journal article

(Version)
Version of Record

(URL)
https://hdl.handle.net/20.500.14094/90000910

Strain Effects on Electronic Bandstructures in Nanoscaled Silicon: From Bulk to Nanowire

Tadashi Maegawa, Tsuneki Yamauchi, Takeshi Hara,
Hideaki Tsuchiya, *Senior Member, IEEE*, and Matsuto Ogawa, *Member, IEEE*

***Abstract*—In this paper, we present a comparative computational study on strain effects in Si nanostructures including bulk, thin film, and nanowire configurations. We employed a first principles calculation to identify the bandstructure parameters such as band splitting energy and transport effective mass. As a result, we found that bulk Si and Si thin film have similar strain effects on the bandstructure parameters under uniaxial ⟨110⟩ strain. Particularly, the effective mass reduction of electrons due to uniaxial ⟨110⟩ strain is expected even in Si thin film. On the other hand, Si nanowire structure with nanoscale cross section has lighter transport effective mass than the other structures, regardless of the amount of uniaxial strain.**

***Index Terms*—Band splitting, bandstructure, effective mass, first principles calculation, quantum confinement, Si nanostructure, strained-Si channel.**

I. Introduction

As THE SIZE of Si-MOSFETs shrinks down to the nanometer scale, new device technologies such as mobility enhanced channels and multigate architectures are strongly needed to realize advanced CMOS devices. Among them, strained-Si channel engineering, which includes the choices of surface orientations, channel directions, strain configurations, and channel materials are recently becoming more important [1]. Particularly, uniaxial strain can be more effective than biaxial strain in increasing the current drive of short-channel devices, because of the effective mass reduction of holes [2], [3] and even electrons [4]. On the other hand, device structures with new gate configurations are preferred to provide better electrostatic control than the conventional planar structures. Thus, ultrathin-body channels and Si nanowire channels with multigate or gate-all-around structures are highly expected.

So far, the effective mass reduction of carriers by applying uniaxial strain has been experimentally demonstrated for bulk-[2]–[4] and ultrathin-body SOI MOSFETs [4]. Understanding of physical mechanisms for such an effective mass reduction in both p- and n-channel MOSFETs has progressed based on theoretical computational studies for bulk-Si MOSFETs [2]–[6]. For ultrathin-body structures, there are few theoretical reports discussing strain effects on the effective mass [7], to the best of our knowledge. However, to further scale down MOSFETs with desired higher performance, an introduction of the strain technology to Si nanostructure channels will be explored in the future.

In this paper, we study strain effects in Si nanostructures, i.e., 2-D thin film and 1-D nanowire, including bulk material. Under extreme scaling of MOSFETs, the number of atoms in the cross section becomes countable, and the consideration of crystal symmetry and bond orientation, in addition to quantum–mechanical confinement is important. Therefore, we employed a first principles method to identify the bandstructure parameters that greatly influence carrier transport properties. For Si nanowires, strain-induced modulation of bandgap and effective mass has been recently reported based on the similar first principles calculations, for various growth directions and cross-sectional shapes and sizes [8]–[10]. In this paper, we intend to highlight its unique strain properties of Si nanowires by comparing with those of bulk and 2-D thin film.

II. Bulk Si

First, we present variations in energy splitting of conduction band edge and effective mass of electrons by applying biaxial and uniaxial strains to bulk Si. Fig. 1 shows the lattice models used in the calculation, where uniaxial strain is parallel to ⟨100⟩ and ⟨110⟩ directions, as shown in Fig. 1(b) and (c), respectively. The plane and directions parallel to strain are uniformly deformed from -1% to 1%, and the lattice constants perpendicular to the strain direction are carefully relaxed. All calculations were performed by using a first principles simulation package, VASP, where the electron–electron exchange and correlation interactions were treated within the generalized gradient approximation. The Kohn–Sham equation was solved by using a plane-wave basis set based on the ultrasoft pseudopotentials and projector-augmented-wave method [11].

Fig. 2(a)–(c) shows the calculated energy splitting of the conduction band edge ΔE_C under biaxial, uniaxial ⟨100⟩, and uniaxial ⟨110⟩ strains, respectively, where energy of the conduction band edge at unstrained condition was set to be zero. The insets show the schematic diagrams of six conduction band valleys on a Si (001) surface, numbered from 1 to 6, and also strain directions. As is well known, the strains cause band splitting of the sixfold degenerate valleys into the twofold (5, 6) and the fourfold (1, 2, 3, 4) valleys, as shown in Fig. 2, the amount of which is the largest for biaxial strain and is the smallest for uniaxial ⟨110⟩ strain. The present results are

Manuscript received August 12, 2008; revised December 29, 2008. First published February 27, 2009; current version published March 25, 2009. This work was supported in part by a NEDO/MIRAI project. The review of this paper was arranged by Editor M. Reed.

The authors are with the Department of Electrical and Electronics Engineering, Graduate School of Engineering, Kobe University, Kobe 657-8501, Japan (e-mail: tsuchiya@eedept.kobe-u.ac.jp).

Digital Object Identifier 10.1109/TED.2009.2014185

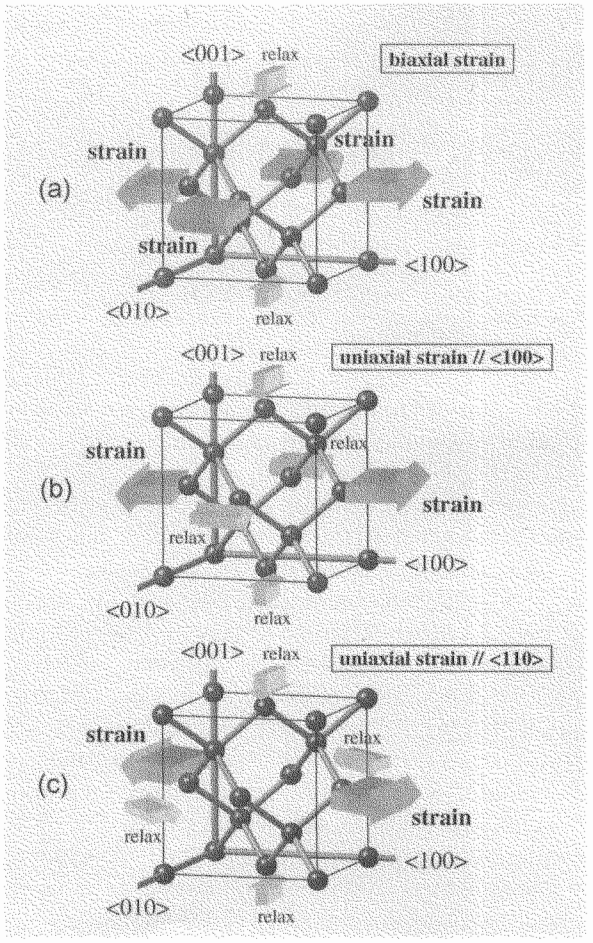

Fig. 1. Lattice models used in the calculation for bulk Si, where (a) biaxial, (b) uniaxial ⟨100⟩, and (c) uniaxial ⟨110⟩ strains. The plane and directions parallel to strain are uniformly deformed from −1% to 1%, and the lattice constant perpendicular to the strain direction is carefully relaxed.

consistent with the previous results based on the empirical nonlocal pseudopotential method by Uchida *et al.* [4] and Ungersboeck *et al.* [6]. Fig. 3 shows the in-plane effective masses computed for the same strain conditions as in Fig. 2. As Uchida *et al.* first demonstrated [4], the m_T reduction and enhancement are observed by applying uniaxial ⟨110⟩ strain, as shown in Fig. 3(c). For comparison purposes, the computed m_T values are compared with those of Uchida *et al.* [4] and Ungersboeck *et al.* [6], as shown in Fig. 4. It is found that the trend of effective mass modulation due to uniaxial ⟨110⟩ strain is the same for both methods, although the present first principles method predicts smaller variation in m_T than the empirical nonlocal pseudopotential method. Therefore, the first principles approach might underestimate the performance enhancement of the strained-Si MOSFETs, and the details are under investigation. In the following sections, we examine the effects of uniaxial ⟨110⟩ strain on Si nanostructures.

III. Silicon 2-D Film

Next, we present the calculated results for Si 2-D film. Fig. 5 shows the unit cells used in the calculation, where we only considered uniaxial strain parallel to ⟨110⟩ direction. Dangling bonds of surface Si's are terminated with hydrogen atoms, and vacuum layers with 0.4 nm thick are added above and below the structure. More realistic models sandwiched between two

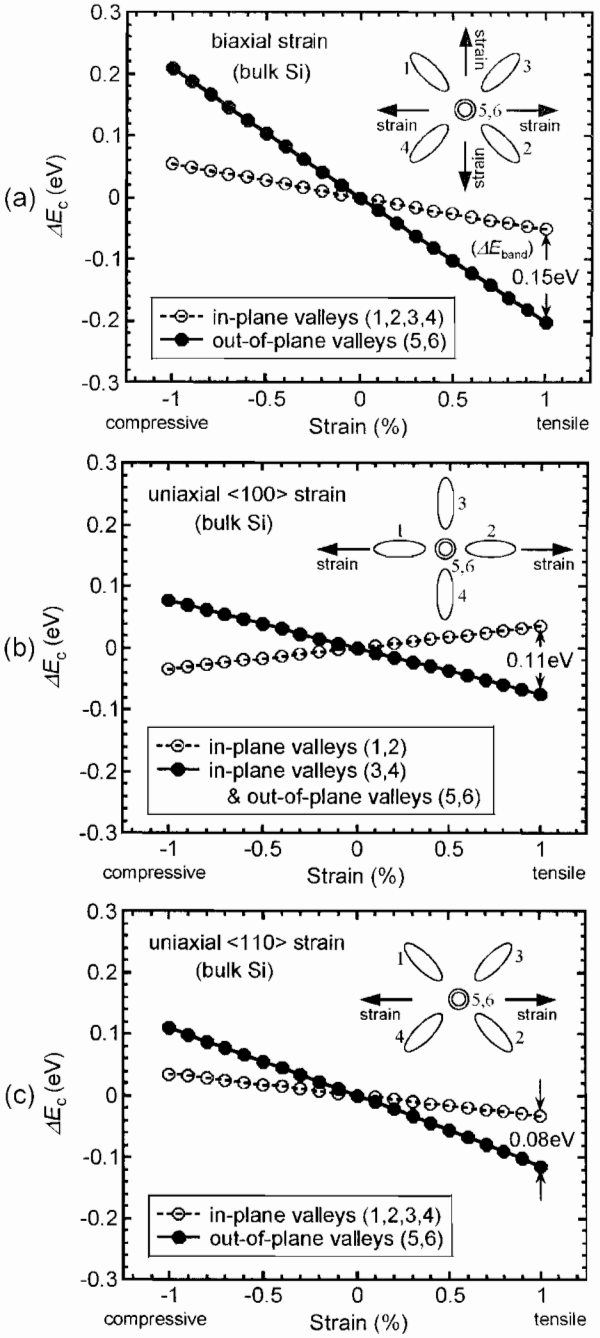

Fig. 2. Calculated energy splitting of conduction band edge ΔE_C under (a) biaxial, (b) uniaxial ⟨100⟩, and (c) uniaxial ⟨110⟩ strains, where the energy of conduction band edge at unstrained condition was set to be zero. The insets show the schematic diagrams of six conduction band valleys on a Si (001) surface, and strain directions.

SiO_2 layers [12] will be applicable to bandstructure calculations under strain. Here, note that the axes in plane perpendicular to confinement direction are ⟨110⟩ and ⟨1$\bar{1}$0⟩ in Fig. 5. The Si thin film consists of five Si atomic layers, which corresponds to Si layer thickness of 0.54 nm. Therefore, electrons confined in the Si thin film are considered to be an ideal 2-D electron gas. Such an extremely scaled SOI-MOSFET with five Si atomic layers was successfully fabricated and its fundamental device operation was also reported [13]. In this paper, we investigate strain effects on such ideal 2-D electron gas.

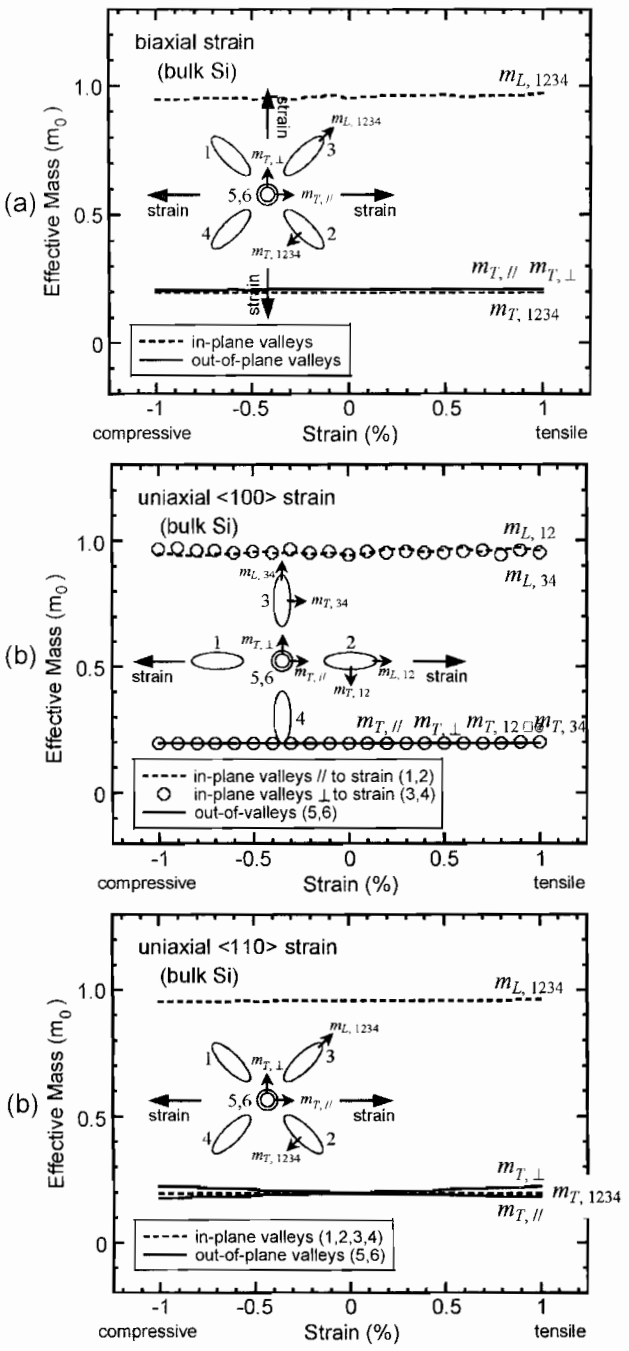

Fig. 3. In-plane effective masses computed for the same strain conditions as in Fig. 2. The m_T reduction and enhancement are observed by applying uniaxial $\langle 110 \rangle$ strain.

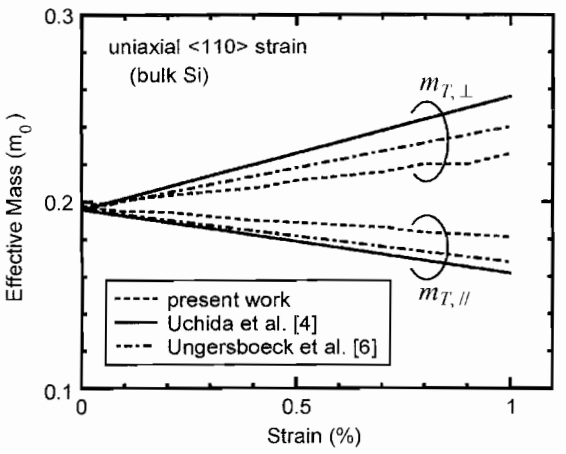

Fig. 4. Comparison of computed m_T values with results from the empirical nonlocal pseudopotential method [4], [6].

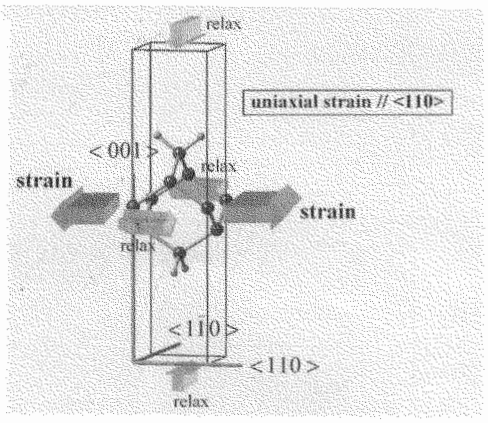

Fig. 5. Unit cells used in the calculation for Si 2-D film, where we considered uniaxial strain parallel to $\langle 110 \rangle$ direction. Dangling bonds of surface Si's are terminated with hydrogen atoms, and vacuum layers are included above and below the structures. Note that the axes in plane perpendicular to confinement direction is $\langle 110 \rangle$ and $\langle 1\bar{1}0 \rangle$. The Si film consists of five Si atomic layers ($T_{\mathrm{Si}} = 0.54$ nm).

Fig. 6 shows the dispersion curves computed for the Si 2-D films, where uniaxial $\langle 110 \rangle$ strain is a) 1% compressive, b) 0%, and c) 1% tensile. Here, note that for all the three dispersions, the energy reference of the vertical axis was set to be the Fermi energy obtained in the case of unstrained Si thin film, to examine quantitative energy splitting of the conduction band edge due to strain as discussed later. From Fig. 6, they have a conduction band minimum at the Γ point, which results from the k-space projection of the two ellipsoidal bands (5, 6) onto the $\langle 001 \rangle$ plane of quantization [14]. There are four more valleys residing off-Γ states (two in the positive and two in the negative k_x axis) that result from the four off-plane ellipsoidal bands (1, 2, 3, 4). The former Γ valleys appear at lower energies because of their heavy quantization mass and have lighter transport mass. On the other hand, the latter off-Γ valleys appear at higher energies because of the lighter quantization mass and have heavier transport mass. In Fig. 6, we note that the twofold Γ valleys are split by the interactions between the two equivalent valleys, which is called "valley splitting [15], [16]." The valley splitting strongly depends on quantization, and the splitting energies in Fig. 6 are found to be far larger than thermal energy $k_B T$. Furthermore, according to our calculation, Si thin film models sandwiched between two SiO_2 layers showed approximately twice larger valley splitting than the hydrogen-terminated model used in this paper [17]. Consequently, the valley splitting can be an important effect that influences, for instance, charge accumulation in ultrathin films and nanowires because the density-of-states at conduction band minimum decreases. Recently, this issue attracts much attention in perspective of I–V characteristics and ballistic injection velocity of Si nanotransistors [18], [19], and of developing Si light emitting devices [20].

It is also found from Fig. 6 that uniaxial $\langle 110 \rangle$ strain causes band splitting between the Γ and off-Γ valleys in Si 2-D film.

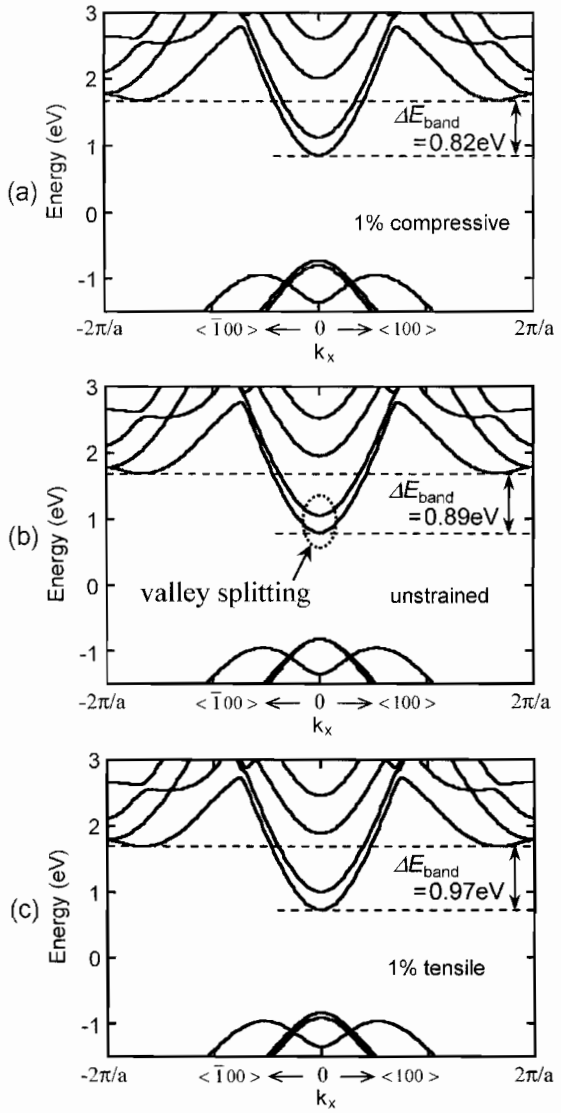

Fig. 6. Dispersion curves computed for Si 2-D film, where uniaxial ⟨110⟩ strain is (a) 1% compressive, (b) 0%, and (c) 1% tensile. Here, the energy reference of the vertical axis was set to be the Fermi energy in the case of unstrained Si thin film.

Then, we plotted the calculated energy splitting of the conduction band edge ΔE_C, as shown in Fig. 7, where the off-Γ valleys have much higher energies due to quantum confinement. We can see that the ground-state Γ valley moves up and down due to uniaxial ⟨110⟩ strain, while the off-Γ fourfold valleys are almost constant. Furthermore, Fig. 8 shows the in-plane effective masses of the ground-state Γ valley. It is found that the m_T reduction and enhancement are expected to occur even in uniaxial ⟨110⟩-strained Si thin film. Indeed, the electron mobility enhancement and reduction under uniaxial ⟨110⟩ strain has been observed experimentally in such ultrathin-body MOSFETs [4], which is attributed to the m_T change due to the uniaxial strain. Based on the above results, Si 2-D film is found to have similar strain effects as in bulk Si under uniaxial ⟨110⟩ strain.

IV. Silicon 1-D Nanowire

Finally, we present the calculated results for Si 1-D nanowire. Fig. 9 shows the simulation model of Si nanowire and its

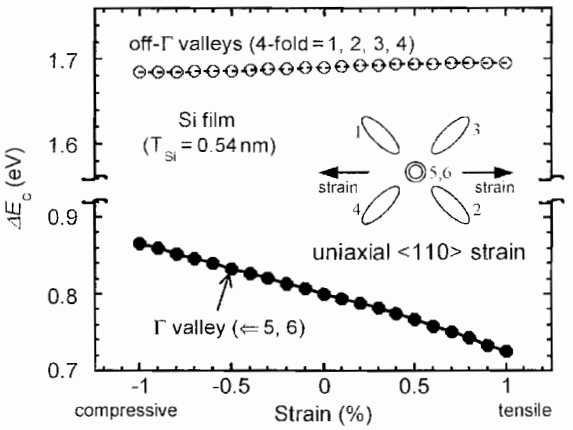

Fig. 7. Calculated energy splitting of Si 2-D film under uniaxial ⟨110⟩ strain, where the off-Γ valleys have much higher energies due to quantum confinement.

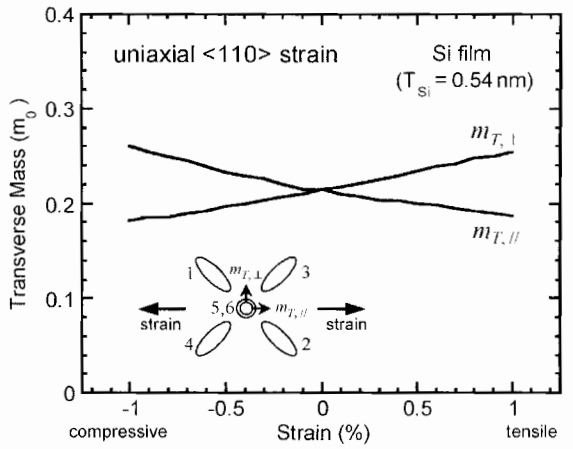

Fig. 8. In-plane effective masses of ground-state Γ valley estimated for Si 2-D film under uniaxial ⟨110⟩ strain. The m_T reduction and enhancement are expected to occur even in Si thin film.

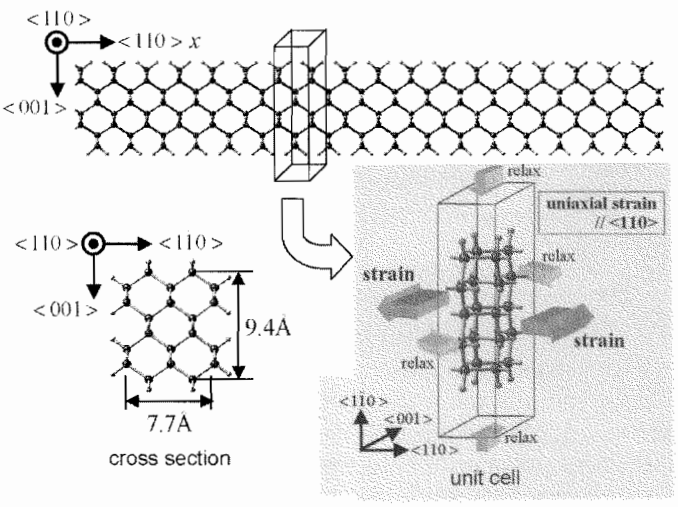

Fig. 9. Simulation model of Si nanowire and its unit cell. Quantum confinement directions are ⟨001⟩ and ⟨1$\bar{1}$0⟩. The nanowire direction was chosen at ⟨110⟩, because a higher current capability compared to other directions as ⟨100⟩ and ⟨111⟩ is expected [14]. Uniaxial strain was applied along ⟨110⟩ direction.

unit cell. As in the Si 2-D film, dangling bonds of surface Si's are terminated with hydrogen atoms, and the nanowire is surrounded by vacuum layers with 0.3 nm thick. Quantum

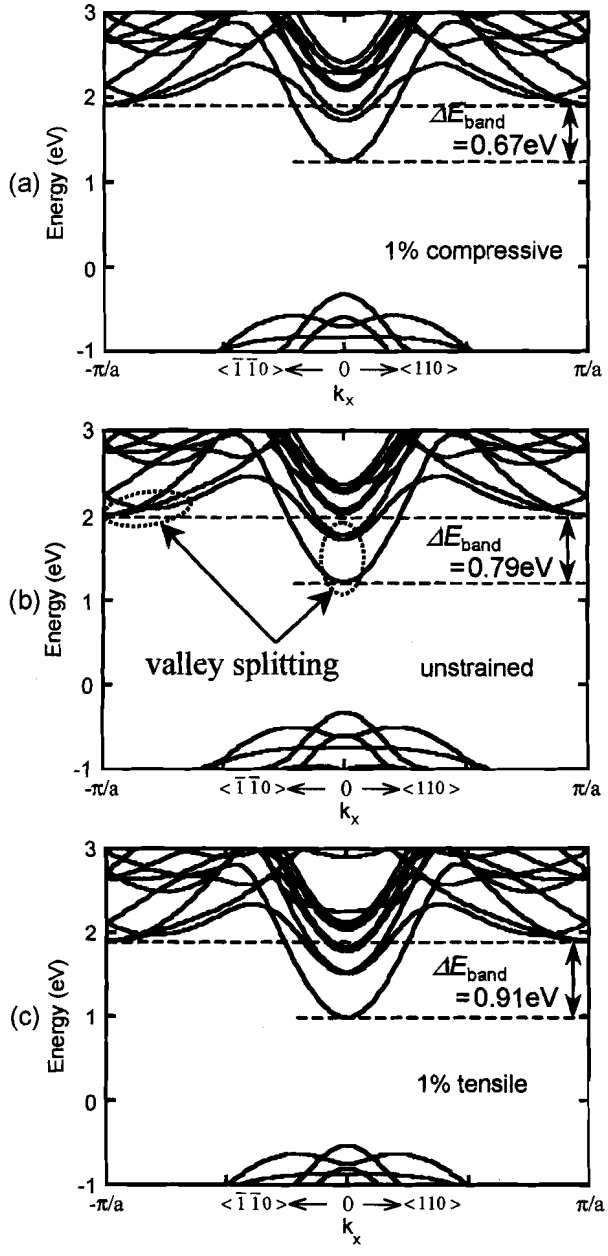

Fig. 10. Dispersion curves computed for ⟨110⟩-oriented nanowire, where uniaxial strain is (a) 1% compressive, (b) 0%, and (c) 1% tensile, where the energy reference of the vertical axis is the Fermi energy in the case of unstrained Si nanowire.

confinement directions are ⟨001⟩ and ⟨1$\bar{1}$0⟩, and their dimensions are 0.94 and 0.77 nm, respectively. Therefore, electrons in the nanowire are considered to be an ideal 1-D electron gas. The nanowire direction was chosen at ⟨110⟩, because a higher current capability compared to other directions as ⟨100⟩ and ⟨111⟩ is expected [14]. In addition, we have to add that relaxed nanowire is 3% stretched along the axis even in the unstrained condition, which agrees well with the previously reported theoretical results [9], [21]. Then, uniaxial compressive and tensile strains were applied along ⟨110⟩ direction.

Fig. 10 shows the dispersion curves computed for the ⟨110⟩-oriented Si nanowires under (a) 1% compressive, (b) 0%, and (c) 1% tensile uniaxial strains, where the energy reference of the vertical axis for all the three dispersions is the Fermi energy

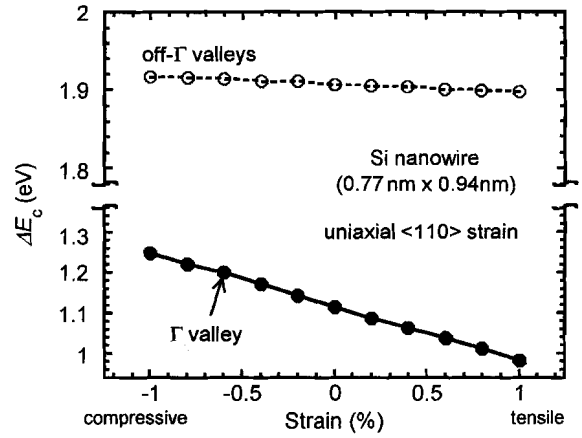

Fig. 11. Calculated energy splitting of Si 1-D nanowire under uniaxial ⟨110⟩ strain.

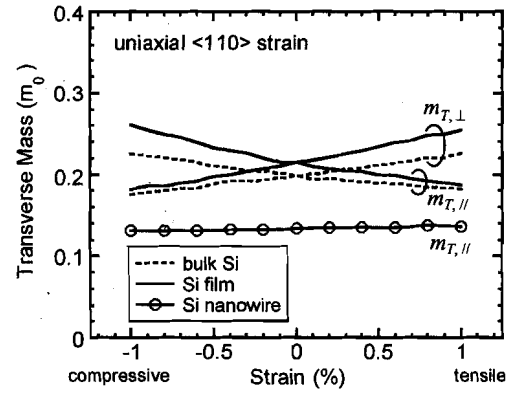

Fig. 12. In-plane effective mass of ground-state Γ valley estimated for Si 1-D nanowire under uniaxial ⟨110⟩ strain. Results for bulk and 2-D film are also plotted for comparison.

in the case of unstrained Si nanowire. Overall features such as conduction band minimum and valley splitting at the Γ point are similar to the Si 2-D film, but furthermore the fourfold off-Γ valleys are found to be split by the valley interactions in the Si nanowire, which results from the k-space projection of the two ellipsoidal bands (1, 4) or (2, 3) onto the ⟨1$\bar{1}$0⟩ plane of quantization [14]. Since the valley splitting depends on quantization, the splitting energies at the Γ point in Fig. 10 are quite larger than those in Fig. 6 for Si 2-D film.

Next, Fig. 11 shows the calculated energy splitting of the conduction band edge ΔE_C. The strain dependence of the conduction band edge is quite similar to the Si 2-D film, although the off-Γ valleys indicate an opposite strain dependence to Fig. 7. The strain dependence of off-Γ valleys in Fig. 11 is different from the previous study [9], [10]. We think it is because we set the energy reference of all the dispersion curves at the Fermi energy in the case of unstrained Si nanowire. Indeed, when the energy offset is not corrected, the same strain dependence of off-Γ valleys as in [9] and [10] is obtained. Fig. 12 shows the in-plane effective mass of the ground-state Γ valley, which is also compared with bulk and 2-D film. It is found that the m_T reduction due to uniaxial ⟨110⟩ tensile strain is not observed, but a smaller m_T is predicted in the Si 1-D nanowire. The present results are consistent with those of [8] and [9]. The estimated transport mass is $\sim 0.13 m_0$ independently of strain,

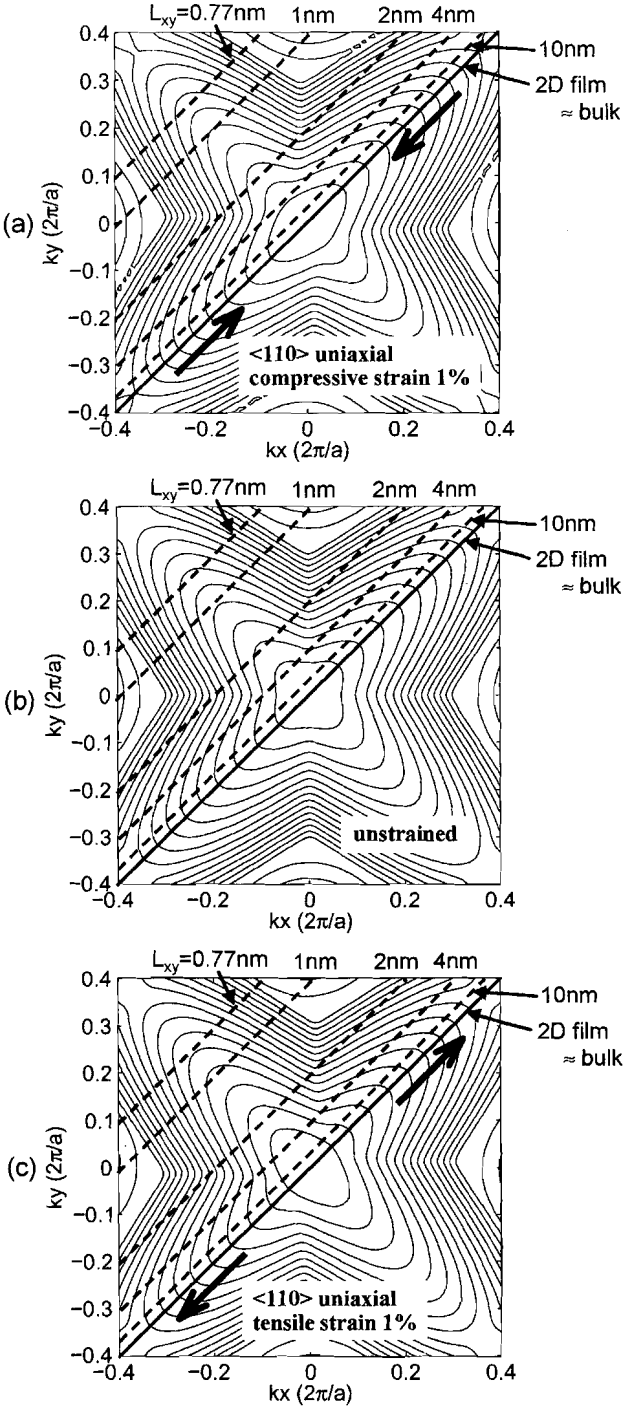

Fig. 13. Energy contours in k_x–k_y plane near conduction band minimum of Si 2-D films under (a) 1% compressive, (b) 0%, and (c) 1% tensile uniaxial strains, where the confinement direction is $\langle 001 \rangle$ and the thickness L_z is taken at 0.94 nm. The dashed lines that cross at 45° represent an extra quantization in the $\langle 1\bar{1}0 \rangle$ -direction in the present nanowire. A line for $L_{xy} = 0.77$ nm corresponds to the present nanowire quantization, and lines for $L_{xy} = 1$ nm, 2 nm, 4 nm, 10 nm, and ∞ (2-D film limit) are also drawn for comparison.

which is smaller by 32% than the bulk m_T. Very recently, such a smaller mass has been reported for unstrained Si nanowires based on the empirical tight-binding band calculation, and its physical mechanism was clearly explained in terms of semi-analytical construction of the nanowire dispersions by using the anisotropy and nonparabolicity in the Si conduction band Brillouin zone [14]. We apply that argument to explain why the effective mass of Si nanowire is independent of the strain, contrary to that of 2-D film as follows. Fig. 13 shows the energy contours in the k_x–k_y plane near the conduction band minimum of Si 2-D films under (a) 1% compressive, (b) 0%, and (c) 1% tensile uniaxial strains, where the confinement direction is $\langle 001 \rangle$ and the thickness L_z is taken at 0.94 nm. Here, note that an extra quantization in the $\langle 1\bar{1}0 \rangle$ -direction takes place in the present nanowire as indicated by the dashed lines that cross Fig. 13 at 45°, where "cut" through the energy contours along those lines semianalytically forms 1-D dispersion curves of the nanowire [14]. In Fig. 13, a line for $L_{xy} = 0.77$ nm, which corresponds to the present nanowire quantization, and also lines for $L_{xy} = 1$ nm, 2 nm, 4 nm, 10 nm, and ∞ (2-D film limit) are drawn for comparison. It is found that higher k_{xy} region has larger curvature of the dispersion and is immune to uniaxial $\langle 110 \rangle$ strain. As a result, the effective mass of the nanowire becomes smaller than those of bulk and 2-D film, and also changes little by uniaxial $\langle 110 \rangle$ strains as found in Fig. 12. However, as the structure becomes thicker in the $\langle 1\bar{1}0 \rangle$ direction, the quantization line moves toward that of 2-D film limit, and its effective mass increases to the bulk transverse mass and a response to the strain is restored as well. The transition from the bulklike properties to the 1-D properties seems to occur when the thickness of the $\langle 1\bar{1}0 \rangle$ direction becomes smaller than 2–4 nm in the present semianalytical description, but a further investigation based on a fully first principles analysis is necessary to clarify such 3-D–1-D transition behavior correctly, which is currently in progress. Leastwise, the $\langle 110 \rangle$-oriented Si nanowire with nanoscale cross section is found to have the unique strain properties, unlike bulk and 2-D film.

V. Conclusion

We have studied strain effects in Si nanostructures based on the first principles calculation. We found that bulk Si and Si 2-D film have similar strain effects on the bandstructure parameters under uniaxial $\langle 110 \rangle$ strain. Particularly, the m_T reduction due to uniaxial $\langle 110 \rangle$ strain is expected even in Si 2-D film. On the other hand, Si 1-D nanowire with nanoscale cross section has lighter m_T than the others, although the m_T change due to uniaxial $\langle 110 \rangle$ strain is not available. Therefore, $\langle 110 \rangle$-oriented Si nanowire has higher injection velocity [14], but it is likely that the decrease in the density-of-state due to the valley splitting may degrade the current capability. Furthermore, the lighter mass can cause a larger source–drain tunneling current at OFF-state of MOSFETs. Therefore, a quantum transport simulator considering the full-band bandstructures designed based on atomistic modeling will be required to assess the performance limits of Si nanowire transistors.

References

[1] S. Takagi, T. Irisawa, T. Tezuka, T. Numata, S. Nakaharai, N. Hirashita, Y. Moriyama, K. Usuda, E. Toyoda, S. Dissanayake, M. Shichijo, R. Nakane, S. Sugahara, M. Takenaka, and N. Sugiyama, "Carrier-transport-enhanced channel CMOS for improved power consumption and performance," *IEEE Trans. Electron Devices*, vol. 55, no. 1, pp. 21–39, Jan. 2008.

[2] S. E. Thompson, G. Sun, K. Wu, J. Lim, and T. Nishida, "Key differences for process-induced uniaxial vs. substrate-induced biaxial stressed Si and Ge channel MOSFETs," in *IEDM Tech. Dig.*, 2004, pp. 221–224.
[3] L. Shifren, X. Wang, P. Matagne, B. Obradovic, C. Auth, S. Cea, T. Ghani, J. He, T. Hoffman, R. Kotlyar, Z. Ma, K. Mistry, R. Nagisetty, R. Shaheed, M. Stettler, C. Weber, and M. D. Giles, "Drive current enhancement in p-type metal–oxide–semiconductor field-effect transistors under shear uniaxial stress," *Appl. Phys. Lett.*, vol. 85, no. 25, pp. 6188–6190, Dec. 2004.
[4] K. Uchida, T. Krishnamohan, K. C. Saraswat, and Y. Nishi, "Physical mechanisms of electron mobility enhancement in uniaxial stressed MOSFETs and impact of uniaxial stress engineering in ballistic regime," in *IEDM Tech. Dig.*, 2005, pp. 135–138.
[5] E. X. Wang, P. Matagne, L. Shifren, B. Obradovic, R. Kotlyar, S. Cea, M. Stettler, and M. D. Giles, "Physics of hole transport in strained silicon MOSFET inversion layers," *IEEE Trans. Electron Devices*, vol. 53, no. 8, pp. 1840–1851, Aug. 2006.
[6] E. Ungersboeck, S. Dhar, G. Karlowatz, H. Kosina, and S. Selberherr, "Physical modeling of electron mobility enhancement for arbitrarily strained silicon," *J. Comput. Electron.*, vol. 6, no. 1–3, pp. 55–58, Sep. 2007.
[7] J. Yamauchi, "Effective mass anomalies in strained-Si thin films and crystals," *IEEE Electron Device Lett.*, vol. 29, no. 2, pp. 186–188, Feb. 2008.
[8] D. Shiri, Y. Kong, A. Buin, and M. P. Anantram, "Strain induced change of bandgap and effective mass in silicon nanowires," *Appl. Phys. Lett.*, vol. 93, no. 7, p. 073 114, Aug. 2008.
[9] P. W. Leu, A. Svizhenko, and K. Cho, "*Ab initio* calculations of the mechanical and electronic properties of strained Si nanowires," *Phys. Rev. B, Condens. Matter*, vol. 77, no. 23, p. 235 305, Jun. 2008.
[10] K.-H. Hong, J. Kim, S.-H. Lee, and J. K. Shin, "Strain-driven electronic band structure modulation of Si nanowires," *Nano Lett.*, vol. 8, no. 5, pp. 1335–1340, May 2008.
[11] G. Kresse and J. Furthmüller, "Efficient iterative schemes for *ab initio* total-energy calculation using a plane-wave basis set," *Phys. Rev. B, Condens. Matter*, vol. 54, no. 16, pp. 11 169–11 186, Oct. 1996.
[12] T. Hara, Y. Yamada, T. Maegawa, and H. Tsuchiya, "Atomistic study on electronic properties of nanoscale SOI channels," *J. Phys. Conf. Series*, vol. 109, p. 012 012, 2008.
[13] K. Uchida, J. Koga, and S. Takagi, "Experimental study on carrier transport mechanisms in double- and single-gate ultrathin-body MOSFETs—Coulomb scattering, volume inversion, and δT_{SOI}-induced scattering," in *IEDM Tech. Dig.*, 2003, pp. 805–808.
[14] N. Neophytou, A. Paul, M. Lundstrom, and G. Klimeck, "Bandstructure effects in silicon nanowire electron transport," *IEEE Trans. Electron Devices*, vol. 55, no. 6, pp. 1286–1297, Jun. 2008.
[15] T. Ando, A. B. Fowler, and F. Stern, "Electronic properties of two-dimensional systems," *Rev. Mod. Phys.*, vol. 54, no. 2, pp. 437–672, Apr. 1982.
[16] A. Rahman, G. Klimeck, M. Lundstrom, T. B. Boykin, and N. Vagidov, "Atomistic approach for nanoscale devices at the scaling limit and beyond—Valley splitting in Si," *Jpn. J. Appl. Phys.*, vol. 44, no. 4B, pp. 2187–2190, Apr. 2005.
[17] T. Hara, "First principles bandstructure calculations of ultrathin SOI channels," M.E. thesis, Grad. School Eng., Kobe University, Kobe, Japan, 2009 (in Japanese).
[18] J. Wang, A. Rahman, A. Ghosh, G. Klimeck, and M. Lundstrom, "On the validity of the parabolic effective-mass approximation for the I–V calculation of silicon nanowire transistors," *IEEE Trans. Electron Devices*, vol. 52, no. 7, pp. 1589–1595, Jul. 2005.
[19] Y. Liu, N. Neophytou, T. Low, G. Klimeck, and M. Lundstrom, "A tight-binding study of the ballistic injection velocity for ultrathin-body SOI MOSFETs," *IEEE Trans. Electron Devices*, vol. 55, no. 3, pp. 866–871, Jun. 2008.
[20] H. Scheel, S. Reich, and C. Thomsen, "Electronic band structure of high-index silicon nanowires," *Phys. Stat. Sol. (B)*, vol. 242, no. 12, pp. 2474–2479, Oct. 2005.
[21] S. You, M. Gao, and Y. Wang, "Band structure of surface terminated silicon nanowire," in *Proc. Extended Abstracts Int. Conf. SSDM*, Tsukuba, Japan, Sep. 2007, pp. 698–699.

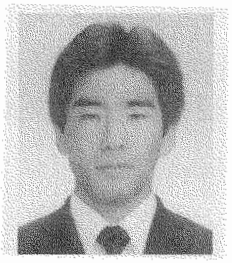

Tadashi Maegawa was born in Kobe, Japan, on May 4, 1983. He received the B.S. degree in electrical and electronics engineering from Kobe University, Kobe, in 2007, where he is currently working toward the M.S. degree.

His research involves first principles simulation of silicon nanowires.

Mr. Maegawa is a member of the Japan Society of Applied Physics.

Tsuneki Yamauchi, photograph and biography not available at the time of publication.

Takeshi Hara was born in Ishikawa, Japan, on July 7, 1984. He received the B.S. degree in electrical and electronics engineering from Kobe University, Kobe, Japan, in 2007, where he is currently working toward the M.S. degree.

His research involves first principles simulation of ultrathin SOI channels, including high-k gate oxide materials.

Mr. Hara is a member of the Japan Society of Applied Physics.

Hideaki Tsuchiya (M'93–SM'01) was born in Ehime, Japan, on August 12, 1964. He received the B.S., M.S., and Ph.D. degrees in electronic engineering from Kobe University, Kobe, Japan, in 1987, 1989, and 1993, respectively.

In 1993, he was with the Department of Electrical and Electronics Engineering, Kobe University, as a Research Associate. He has been engaged in research of quantum transport simulation of mesoscopic devices. From 1999 to 2000, he was a Visiting Scientist with the University of Illinois, Urbana–Champaign, IL. Since 2003, he has been an Associate Professor with the Graduate School of Engineering, Kobe University. His current research includes the quantum transport modeling of nanoscale MOSFETs and the first principles simulation of atomic-scale devices.

Dr. Tsuchiya is a member of the Institute of Electronics, Information and Communication Engineers of Japan, and the Japan Society of Applied Physics. He received a Young Scientist Award in 1998 from the Japan Society of Applied Physics and an Outstanding Achievement Award for a pioneering research on nanoscale device simulator in 2006 from the Institute of Electronics, Information and Communication Engineers of Japan.

Matsuto Ogawa (M'80) received the B.E. degree in electrical engineering and the M.S. and Ph.D. degrees in electronic engineering from the University of Tokyo, Tokyo, Japan, in 1980, 1982, and 1985, respectively.

In that year, he became a Research Associate with the Department of Electronic Engineering, Kobe University, Kobe, Japan, where he is currently a Full Professor. He has been engaged in research of lightwave electronics and nanoscaled devices. His current research includes quantum transport modeling in nanostructures. From 1992 to the end of 1993, he was on leave with IBM T.J. Watson Research Center, NY, as a Visiting Scientist.

Dr. Ogawa is a member of the Japan Society of Applied Physics and the Institute of Electronics, Information and Communication Engineers (IEICE) of Japan. He received Electronics Society Award in 2006 from the IEICE and Project Research Award from the Semiconductor Technology Academic Research Center in 2008.